NIPPON STEEL TECHNICAL REPORT No. 95 January 2007

UDC 621 . 791 . 053 : 539 . 531 : 669 . 784

Carbon Equivalent to Assess Hardenability of Steel and Prediction of HAZ Hardness Distribution

Tadashi KASUYA*1 Yuji HASHIBA*1

Abstract

A practical method to predict HAZ hardness distribution was studied by considering the effect of prior austenite grain sizes on hardenability and that of tempering. For 400 to 490MPa grade steels, hardness distribution between fusion and Ac_3 lines can be fairly well predicted by introducing the effect of grain sizes to the maximum HAZ hardness prediction method. For boron added 780MPa grade steel, since the maximum hardness is obtained at the area a little bit away from the fusion line, the present method cannot predict its HAZ hardness well. Hardness at Ac_1 line can be evaluated with the tempering parameter.

1. Introduction

To evaluate hardenability, which is an important metallurgical characteristic of steel, two kinds of indices have been proposed: the ideal critical diameter (or the hardenability-multiplying factor expressing it) [1] and the carbon equivalent [2, 3].

The ideal critical diameter is the maximum diameter of a round bar specimen that can be quenched to the center under the condition of ideal quenching (assuming an infinite cooling capacity at the surface), and a specimen is judged to be quenched to the center when the fraction of martensite at the center is 50% or more (100% in some cases). It is easy to understand that when quenching a steel bar, the larger its diameter the more difficult it is for the center portion to transform into martensite. This means that a steel whose ideal critical diameter is larger can transform into martensite more easily.

The carbon equivalent is an indicator expressing the critical cooling time required for a steel material to change into 100% martensite. The carbon equivalent was initially used to express not the critical cooling time but the critical cooling rate [3], but it is presently used to express the critical cooling time because the cooling time from 800 to 500℃ was used for an equation to calculate the hardness of a heat-affected zone (HAZ) of a weld joint [4]. If the cooling time after welding a steel is shorter than the critical cooling time, the structure of a HAZ turns into 100% martensite, and otherwise, the structure of a HAZ may contain phases other than martensite. This means that a steel having a long critical cooling time undergoes martensitic transformation easily.

As explained above, both the ideal critical diameter and carbon equivalent are indicators of how easily a steel undergoes martensitic transformation, and thus their metallurgical meanings are considered the same. The interrelation between them has been made clear through application of heat transfer analysis [5].

One of the differences between these indicators, on the other hand, is whether the influence of austenitic grain size is taken into consideration; whereas the equation for calculating the ideal critical diameter includes a term of the hardenability-multiplying factor based on austenitic grain size, the equation for the carbon equivalent usually does not include a term of grain size or diameter. The ideal critical diameter is used mainly for heat treatment of a steel material, and the carbon equivalent for evaluating a HAZ. However, this does not mean that the hardenability of a HAZ does not depend on the austenitic grain size: in fact, hardness distribution measurement of a HAZ shows that hardness tends to decrease as the distance from the fusion line increases.

A reason why the influence of the austenitic grain size has not been taken into consideration in calculating the carbon equivalent is presumably that the portion that poses problems regarding the properties of a HAZ is the coarse-grain portion near the fusion line, and because the carbon equivalent was initially used for evaluating the properties of that portion, the maximum heating temperature could be considered roughly constant to be just below the melting tem-

*1 Steel Research Laboratories

perature of steel regardless of welding conditions. On the other hand, since the maximum heating temperature in heat treatment of a steel material depends on the condition of the process, the hardenability-multiplying factor that expresses the influence of crystal grain size was introduced into the calculation of the ideal critical diameter as a matter of course.

In consideration of the above, in the first place in the present study, an attempt was made to introduce a term expressing the influence of the austenitic grain size into the formula of the carbon equivalent. Our method of introducing the term in the present study was to calculate a carbon equivalent using the equation that Kirkaldy et al.[6] proposed for estimating the incubation time until a transformation product began to form, which the equation took the influence of grain size into consideration. In consideration of the equation of Kirkaldy et al., herein is a discussion of how the equations including a grain-size term for calculating the carbon equivalent should be. Then based on the findings reached through the discussion, an attempt was made to construct equations for estimating the hardness distribution of a HAZ. A reason why the hardness inside a HAZ is not uniform is presumably that the austenitic grain size is different at different portions of a HAZ and this causes difference in hardenability. This seems to indicate that, if the influence of the austenitic grain size is included in the calculation of the carbon equivalent, it may be possible to formulate equations to estimate the hardness distribution of a HAZ.

2. Calculation of Carbon Equivalent

The method for calculating the carbon equivalent from the estimation equation of the incubation time is discussed in this section. The basic rule used here is the additivity rule[7]. According to the additivity rule, letting τ be the incubation time until a certain transformation takes place, which depends on temperature, and dividing a welding cooling curve into a step function, when the time interval of each step of the function is dt, then the fraction of the incubation time that has passed during a step is expressed as dt/τ, and when the integration of dt/τ becomes 1, a transformation is considered to have occurred. (By the way, this reasoning is sometimes used for converting a TTT diagram into a CCT diagram.) According to the above reasoning, the condition under which a transformation does not take place is expressed as follows:

$$\int_0^{t_e} \frac{dt}{\tau} \leq 1 \qquad (1)$$

When a cooling process ends while the value of the left-hand side of Equation (1) is 1 or less, then the microstructure of the material is 100% martensite. From this equation, it is possible to calculate the critical cooling time in which the value of the left-hand side is equal to 1; in the integration, $t = 0$ when the temperature T of a weld joint reaches the Ae_3 temperature, and $t = t_e$ when T reaches Ms. The cooling curve I in **Fig. 1** corresponds to the case where the value of Equation (1) is equal to 1. Fig. 1 is a CCT diagram and this cooling curve in the graph corresponds to the critical cooling time in which the structure of a HAZ becomes 100% martensite. This means that the critical cooling time (Δt_M in Fig. 1), in which the microstructure of the HAZ becomes 100% martensite, is defined as the cooling time from 800 to 500°C along the cooling curve corresponding to the value of left-hand side of Equation (1) being 1. If the incubation time τ is given as a function of the chemical composition of the material, it will be possible to define a carbon equivalent using the function and Equation (1). If, in addition, the formula that defines

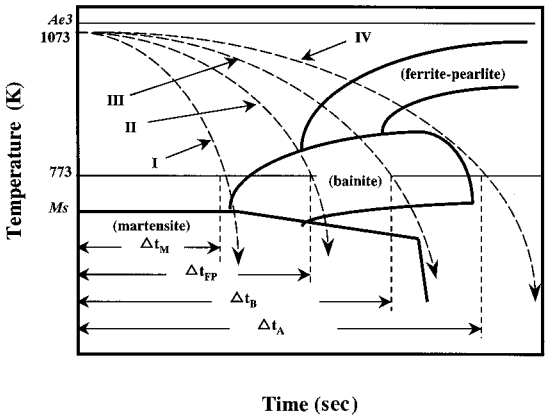

Fig. 1 Critical cooling curves and cooling times in the CCT diagram

τ includes a term of the influence of austenitic grain size, it will be possible to make the carbon equivalent reflect the influence of the grain size.

Then, the method for actually calculating Equation (1) is briefly explained. Because the object of the calculation here is to examine how a formula to evaluate Δt_M is expressed using the chemical composition of the material in question, Equation (1) is modified into Equation (3) using Equation (2), thus:

$$\int_0^{t_e} \frac{dt}{\tau} = \int_{Ae_3}^{Ms} \frac{1}{\tau}\left(\frac{dt}{dT}\right) dT = 1, \qquad \frac{dt}{dT} \approx \frac{\Delta t_M}{300} \qquad (2)$$

$$\Delta t_M = \frac{300}{\int_{Ae_3}^{Ms} \frac{dT}{\tau}} \qquad (3)$$

So far, the carbon equivalent for evaluating the hardenability of a HAZ has been defined as follows:

$$1n(\Delta t_M) = A \cdot CE_M + B \qquad (4)$$

where, A and B are constants, and the subscript M of the carbon equivalent CE means martensite. Equation (3) yields the following equation:

$$1n\,(\Delta t_M) = 1n\,(300) - 1n\left(\int_{Ae_3}^{Ms} \frac{dT}{\tau}\right) \qquad (5)$$

Comparing Equation (4) with Equation (5), one can understand that the carbon equivalent corresponds to the linear terms that are obtained when the second term of the right-side of Equation (5) is expressed in the Taylor series.

When the second term of Equation (5) is expressed in the Taylor series with respect to each element, the linear coefficient (A_x) of each term is expressed as follows:

$$\begin{aligned} A_X &= \frac{\partial}{\partial X}\left[1n\left(\int_{Ae_3}^{Ms} \frac{dT}{\tau}\right)\right] \\ &= \frac{1}{\left(\int_{Ae_3}^{Ms} \frac{dT}{\tau}\right)}\left[-\int_{Ae_3}^{Ms} \frac{1}{\tau^2}\left(\frac{\partial \tau}{\partial X}\right) dT - \frac{1}{\tau_{Ae_3}}\frac{\partial Ae_3}{\partial X} + \frac{1}{\tau_{Ms}}\frac{\partial Ms}{\partial X}\right] \\ &= \frac{1}{\int_{Ae_3}^{Ms} \frac{dT}{\tau}}\left[-\int_{Ae_3}^{Ms} \frac{1}{\tau^2}\left(\frac{\partial \tau}{\partial X}\right) dT\right] \end{aligned} \qquad (6)$$

where, τ_{Ae3} is the value of τ when $T = Ae_3$, and τ_{Ms} is that when $T = Ms$, and their values are assumed to be ∞ in the equation modification.

When the calculation of Equation (6) is conducted, the carbon equivalent is determined as follows:

$$\begin{aligned} 1n(\Delta t_M) &= 1n(300) - \{A_C \cdot (C - C_0) + A_{Si} \cdot (Si - Si_0) + A_{Mn} \cdot (Mn - Mn_0) + \cdots\} \\ &= C_0 - A_C \cdot CE_M \end{aligned} \tag{7}$$

where,

$$C_0 = 1n(300) + A_C \cdot C_0 + A_{Si} \cdot Si_0 + A_{Mn} \cdot Mn_0 + \cdots$$
$$CE_M = C + \frac{A_{Si}}{A_C} Si + \frac{A_{Mn}}{A_C} Mn + \cdots$$

and X_0 is the element amount with respect to which Taylor's expansion is done. CE_M in Equation (7) is the carbon equivalent. The value of CE_M will be calculated according to the above calculation method in the following section.

3. Calculation of Carbon Equivalent Using Literature Data

To calculate the value of CE_M using Equation (7), the values of τ, Ae_3 and Ms must be given; the following equations were used [6, 8]:

$$\tau = \frac{\exp(83500 / RT)}{2^{N/8} (Ae_3 - T)^3} (60C + 90Si + 160Cr + 200Mo) \tag{8}$$

$$Ae_3 = 1185 - 203\sqrt{C} - 15.2Ni + 44.7Si + 104V + 31.5Mo + 13.1W - 30Mn - 11Cr - 20Cu + 700P + 400Al + 120As + 400Ti \tag{9}$$

$$Ms = 831 - 474C - 33Mn - 17Ni - 17Cr - 21Mo \tag{10}$$

In the above expressions, the unit of temperature is Kelvin (K), N is the grain size number according to ASTM, and R is gas constant (8.31 $J \cdot mol^{-1} K^{-1}$).

Then, as for the point where Taylor's expansion is conducted, we adopted the average values of chemical compositions of the Kirkaldy's experiments [6] as follows:

$$\begin{aligned} &C_0 = 0.46, \quad Si_0 = 0.23, \quad Mn_0 = 0.78, \quad Ni_0 = 0.27, \\ &Cr_0 = 0.26, \quad Mo_0 = 0.10, \quad Cu_0 = 0.10 \end{aligned} \tag{11}$$

The integration of Equation (6) can be conducted using the above figures. When the coefficients are determined, the carbon equivalent can be calculated from Equation (7). The carbon equivalent thus calculated is as follows:

$$CE_{M\,cal} = C + \frac{Si}{38} + \frac{Mn}{6.0} + \frac{Ni}{12} + \frac{Cr}{1.8} + \frac{Mo}{2.3} + \frac{Cu}{9.1} \tag{12}$$

Table 1 shows the calculation results of the coefficients.

Equation (12) does not contain a term of austenitic grain size. Instead, since Equation (8) indicates that τ depends on N, a term of austenitic grain size was introduced into Equation (12).

Applying Equation (6) to N, the following results were obtained:

$$A_N = \frac{\partial}{\partial N} \left[1n \left(\int_{Ae_3}^{Ms} \frac{dT}{\tau} \right) \right] = \frac{\partial}{\partial N} \left[1n \left(2^{N/8} \right) \right] = \frac{1n(2)}{8} \tag{13}$$

Different from the coefficients of steel chemical compositions, the value of this equation does not depend on the point where the Taylor expansion is conducted, because the dependency of τ on N in Equation (8) is expressed to be separable. It should be noted that, for introducing A_N to the calculation of a carbon equivalent, its ratio to A_C becomes important. This ratio is given below.

Table 1 Summary of coefficients of alloy elements in carbon equivalent

Element	A_x	A_x/A_c	*CE* (Bastien)	*CE* (Yurioka)
		CE_{cal} (Eq.(12))	(Ref.(3))	(Ref.(9))
C	– 3.02	1	1	1
Si	– 0.08	1/38	-	1/24
Mn	– 0.50	1/6.0	1/4.1	1/6.0
Ni	– 0.25	1/12	1/7.9	1/12
Cr	– 1.64	1/1.8	1/8.5	1/8.0
Mo	– 1.30	1/2.3	1/6.5	1/4.0
Cu	– 0.33	1/9.1	-	1/15
N *1)	0.087	– 1/35	-	-

*1) : ASTM grain number

$$A_N / A_C = -\frac{1}{35} \tag{14}$$

The value of Equation (14) is negative, although all the coefficients of the alloying elements are positive as seen in Equation (12). This means that the hardenability decreases as N increases. An increase in the value of N means that the number of grains in a unit area is larger, or the grains are finer; this agrees with the conventional knowledge that the hardenability decreases with finer grains.

For reference purposes, **Table 1** also includes the coefficients [3, 9] of the carbon equivalent for evaluating the hardenability of a HAZ obtained from our experimental results. They agreed well with the results of the present study, which attests to the validity of the present calculation method.

4. Fundamental Study of Formulae to Estimate Hardness Distribution

The descriptions in the preceding section confirmed that the carbon equivalent (hardenability carbon equivalent) to express the critical cooling time required for a steel material to achieve 100% martensite, which is calculated using the additivity rule from the incubation time estimation formula of Kirkaldy et al., agreed well with the carbon equivalent obtained from the experimental results, and this shows the validity of the present study. From this result, to introduce a term that accounts for the influence of austenitic grain size into the carbon equivalent, a term of ASTM grain size number as expressed in Equation (14) should be added. This means that, for both Equations (4) and (8) to hold without mutual conflict, the following substitution is required only:

$$CE_M \rightarrow CE_M - \frac{N}{35} \tag{15}$$

However, Equation (15) in this form is not easy to handle because the ASTM grain size number appears as a variable. To solve this problem, the equation was modified into a form easier to operate in the manner described below.

First, to replace the grain size number with a cooling curve, consideration was given to the following grain growth equation:

$$\frac{dg}{dt} = \frac{k}{g^m} \exp\left(-\frac{Q}{RT} \right) \tag{16}$$

where, g is the grain size (mm), Q is the activation energy in grain growth, T is temperature (K), t is time (s), and m and k are constants.

N is defined by the following equation using the number of grains n per mm^2:

$$n \equiv 8 \cdot 2^N = \frac{1}{\pi(g / 3.552)^2} \tag{17}$$

Note that, Equation (17) is based on the fact that a two-dimensional grain diameter is expressed as g/1.776, g being a three-dimensional grain diameter. Conveniently, Equation (16) is separable, and substituting Equation (16) into Equation (15) using Equation (17), the following equation was obtained:

$$CE_M \rightarrow CE_M + C_{M1} + C_{M2} \ln (I + C_{M3}), \quad I = \int \exp(-Q / RT)\, dt \tag{18}$$

This integration I is the same as that Ashby and Easterling [10] used for evaluating the grain growth in a HAZ; they call it the kinetic strength of heat cycles. Equation (18) includes C_{M1}, C_{M2} and C_{M3} as constants, which depend on m, k, g_0 (initial grain size) and the coefficient of N, but different researchers give them different values in their reports; for example, Ion et al.[11] reported m = 1 while Igawa et al.[12] proposed m = 3. In view of this, the constants in Equation (18) were treated as the parameters to fit the calculation results to the experimental results, assuming the mathematical form of Equation (18).

Besides the above, when Equation (18) is applied to the area near the fusion line, it has to agree with conventional hardness estimation formulae. Furthermore, to make a formula for hardness distribution prediction, it is necessary to consider not only martensite but also bainite and ferrite-pearlite, and for this end, the other three critical cooling times given in Fig. 1 are necessary, namely, the critical cooling time Δt_{FP} for ferrite-pearlite to begin to transform for the first time, the critical cooling time Δt_B for martensite to become 0%, and the critical cooling time Δt_A for ferrite-pearlite to become 100%. If the values of the three constants in Equation (18) are determined experimentally, then it will be possible to take the influence of austenitic grain size into consideration in calculating the carbon equivalents of the above critical cooling times. (Note that the three constants will correspond to the critical cooling times, Δt_{FP}, Δt_B and Δt_A, when their subscripts M are substituted by FP, B and A, respectively.)

Here, before determining the critical cooling times, let us study how the volume fractions of these microstructures are expressed when the cooling times are given. Letting the volume fractions and hardness values of microstructures be V_M (volume fraction of martensite), H_M (hardness of 100% martensite), V_B (volume fraction of bainite), H_B (hardness of 100% bainite), V_{FP} (volume fraction of ferrite-pearlite), H_{FP} (hardness of 100% ferrite-pearlite), then the hardness of a HAZ H_V will be expressed as follows:

$$H_V = H_M \cdot V_M + H_B \cdot V_B + H_{FP} \cdot V_{FP} \tag{19}$$

Many formulae for predicting the maximum hardness so far proposed include terms accounting for volume fractions of these microstructures, but by our experience, the estimation accuracy of the one Yurioka et al. proposed [9] was the best among them. According to their prediction formula, the volume fraction of martensite V_M is estimated as:

$$V_M = 0.5 - 0.455 \cdot \arctan\left\{4\frac{\log(\Delta t_{8/5} / \Delta t_M)}{\log(\Delta t_B / \Delta t_M)} - 2\right\} \tag{20}$$

where, $\Delta t_{8/5}$ is the cooling time determined according to actual welding conditions. The prediction formula of Yurioka et al. does not deal with the volume fractions of bainite and ferrite-pearlite separately. This is presumably because the object of their prediction formula is to obtain a maximum hardness, and once the volume fraction of martensite is given, the maximum hardness can be calculated with a sufficiently good accuracy.

In predicting hardness distribution, however, since austenitic grain size may vary and hardenability is low at portions where the grain size is small, the volume fractions of bainite and ferrite-pearlite are important. For this reason, the following equation was used to express the volume fraction of ferrite-pearlite in a manner similar to Equation (20):

$$V_{FP} = 0.5 + 0.455 \cdot \arctan\left\{4\frac{\log(\Delta t_{8/5} / \Delta t_{FP})}{\log(\Delta t_A / \Delta t_{FP})} - 2\right\} \tag{21}$$

Once the volume fractions of martensite and ferrite-pearlite are given, the volume fraction of bainite V_B is given by the following equation:

$$V_B = 1 - V_M - V_{FP} \tag{22}$$

Hence, when the four critical cooling times (Δt_M, Δt_{FP}, Δt_B and Δt_A) are calculated, the volume fractions of the microstructures are calculated from Equations (20) to (22), and when their hardness values (H_M, H_B and H_{FP}) are given, the hardness of a HAZ can be predicted using Equation (19).

5. Test Results and Predictions of Hardness Distribution Estimation

5.1 Experimental procedure and results

Six kinds of specimen steels shown in **Table 2** were welded by the methods and the conditions given in **Table 3**, and measured hard-

Table 2 Chemical compositions of tested steels

Steel	C	Si	Mn	Ni	Cr	Mo	Cu	Nb	V	B	N	Hv *1)	T_{Ac_1} *2)	T_{Ac_3} *3)
A	0.149	0.20	0.95	0.016	0.018	-	0.005	0.001	0.002	0.0001	0.0028	131	1011	1127
B	0.17	0.37	1.35	0.018	0.027	0.002	0.006	0.002	0.005	0.0003	0.0018	160	1006	1116
C	0.145	0.26	1.16	0.021	0.046	0.002	0.007	0.002	0.001	0.0002	0.004	163	991	1110
D	0.06	0.25	1.3	0.33	0.027	0.003	0.30	0.009	0.002	0.0003	0.0027	170	990	1139
E	0.149	0.21	1.11	0.021	0.023	0.002	0.008	0.007	0.001	0.0002	0.0014	165	984	1105
F	0.149	0.30	0.85	0.83	0.53	0.48	0.23	0.004	0.047	0.0021	0.0109	295	1029	1189

*1): Hardness of the base metal (Vickers scale, 5 kg loading)
*2): Ac_1 temperature [K] using Eq.(9)
*3): Ac_3 temperature [K] using Eq.(3)

Table 3 Welding conditions

Method		Current (A)	Voltage (V)	Speed (mm/s)	Heat input (J/mm)	No.
SMAW		150	27	4.75	852	I
SMAW		170	27	2.5	1836	II
SMAW		220	27	1.83	3240	III
SMAW		285	31	1.83	4819	IV
SAW	L	1060	36	8.67	8285	V
	T	850	40			

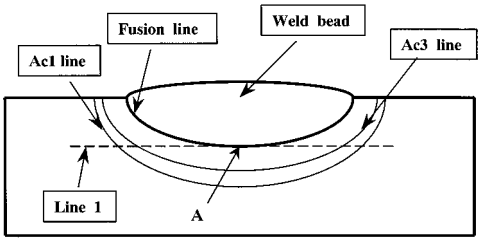

Fig. 2 Schematic illustration of hardness distribution measurement

ness distribution along Line 1 in **Fig. 2**. Steel A was of a 400-MPa class, Steels B to E a 490-MPa class, and Steel F a 780-MPa class. Four different welding conditions were adopted for shielded metal arc welding (SMAW), and one for two-electrode submerged arc welding (SAW). Whereas the SMAW was conducted by the bead-on-plate method, the SAW was conducted with a V groove. The welding consumables used were AWS A5.1 E7016 for the SMAW, and AWS A5.23 F8A8-EG-G for the SAW for all the specimen steels. The Ac_1 and Ac_3 lines in Fig. 2 were defined through microstructural observation. The hardness was measured in Vickers scale with a load of 5 kg.

Figs. 3 to 8 show the hardness distributions of the specimen steels welded under the conditions given in Table 3. Parts (a) to (e) of Figs. 3 to 8 correspond to the welding conditions of Nos. I to V in Table 3, respectively. The solid circles in the graphs represent the test results actually measured. The graphs show that the highest hardness of a HAZ tended to appear near the fusion line just below the weld bead. This is because the maximum heating temperature was highest there, the growth of austenitic grains accelerated, and hardenability of the portion increased. Steels A and B, which were conventionally rolled steels, did not exhibit any softening of HAZs, and the hardness distribution was measured up to the Ac_3 line. In contrast, Steels C to F exhibited softening of HAZs, and the hardness distribution was measured up to the Ac_1 line.

5.2 Formulation of equations for hardness distribution prediction

The mathematical forms for predicting hardness distribution were roughly determined in Section 4. To actually calculate hardness distribution, however, other parameters have to be expressed as the functions of steel chemical compositions. In the first place, as the value of the activation energy for austenitic grain growth necessary for the integration in Equation (18), the following was used.

$$Q = 240{,}000 \text{ (J/mol)}^{10)} \quad (23)$$

Next, as the coefficients for the alloying elements in CE_M, the following was used in accordance with the hardness estimation formula of Yurioka et al..

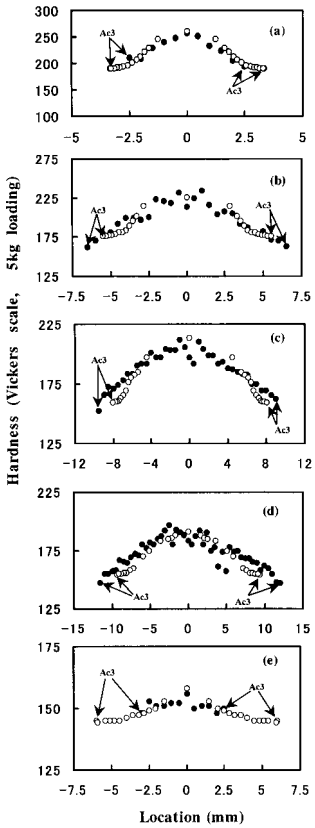

Fig. 3 Experimental (●) and calculated (○) results of hardness distribution in Steel A

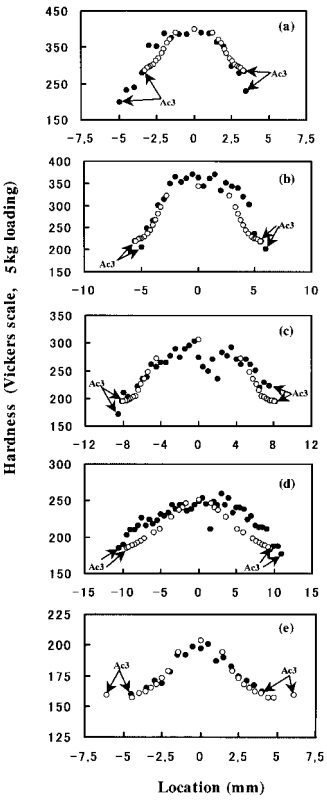

Fig. 4 Experimental (●) and calculated (○) results of hardness distribution in Steel B

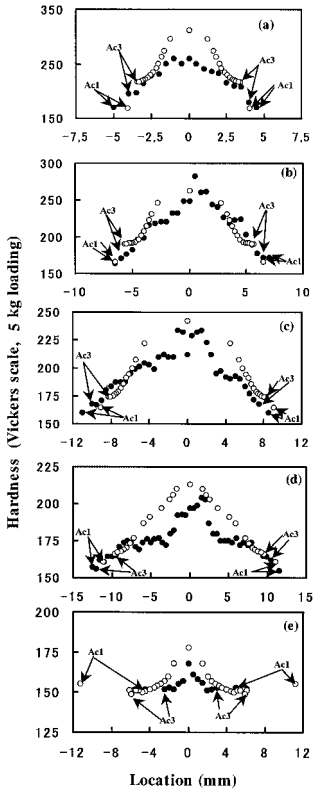

Fig. 5 Experimental (●) and calculated (○) results of hardness distribution in Steel C

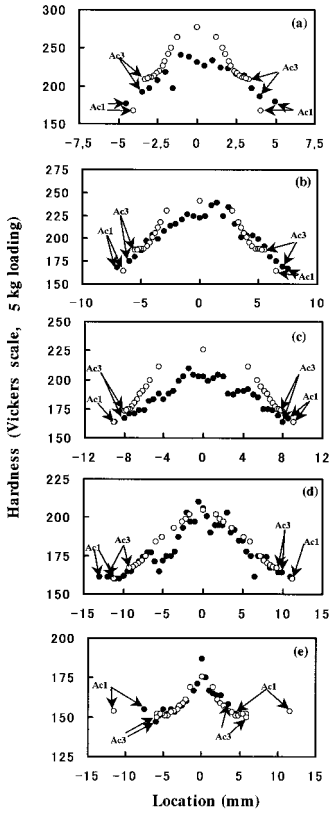

Fig. 6 Experimental (●) and calculated (○) results of hardness distribution in Steel D

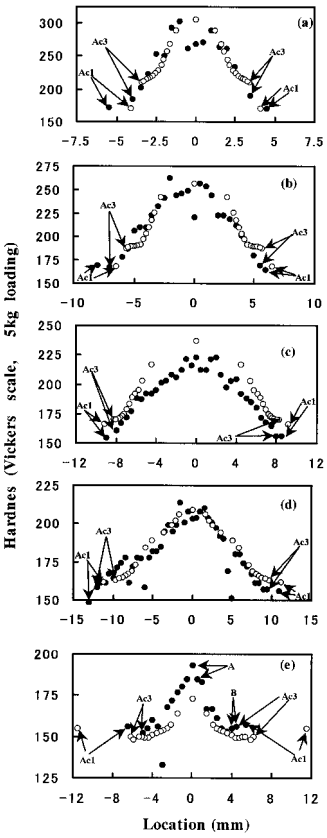

Fig. 7 Experimental (●) and calculated (○) results of hardness distribution in Steel E

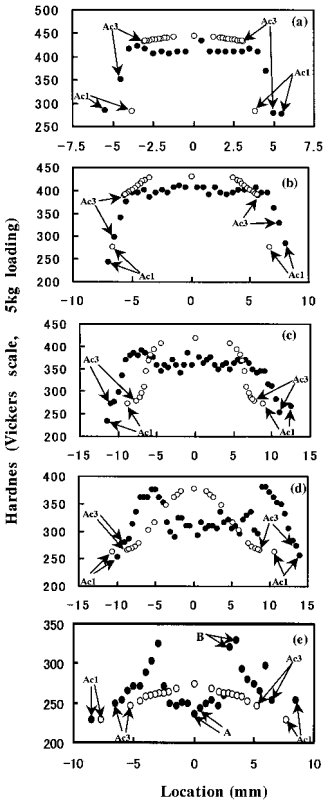

Fig. 8 Experimental (●) and calculated (○) results of hardness distribution in Steel F

$$\begin{aligned}
&1\mathrm{n}(\Delta t_M) = 10.6CE_M - 4.8,\\
&CE_M = C + \frac{Si}{24} + \frac{Mn}{6} + \frac{Cu}{15} + \frac{Ni}{12} + \frac{Mo}{4}\\
&\qquad + \frac{Cr\left(1 - 0.16\sqrt{Cr}\right)}{8} + \Delta H + 0.00585 \cdot 1\mathrm{n}(I')\\
&I' = 2 \times 10^6\left\{I + 1.25 \times 10^{-9}\right\}\\
&\Delta H = \begin{cases} 0, & B \le 0.0001 \\ 0.03 f_N, & B = 0.0002 \\ 0.06 f_N, & B = 0.0003 \\ 0.09 f_N, & B \ge 0.0004 \end{cases} \qquad f_N = \frac{0.02 - N}{0.02}
\end{aligned} \tag{24}$$

Here, let us explain the above equations in a little more detail. All these equations are identical to the original ones Yurioka et al. proposed except for the integral term (I') of CE_M. The object of the present study is to introduce the influence of austenitic grain size into the calculation of a carbon equivalent, and not to reevaluate the coefficients of alloying elements, and for this reason, only the integral term was added anew. Note that the integral term in Equation (24) is such that the value of the equation is nearly zero when it is calculated according to the thermal history at a fusion line. In other words, Equation (24) was so formulated as to agree with the hardness prediction formula of Yurioka et al. at a fusion line. Besides this, as will be explained later, the coefficient of I', 0.00585, was determined so that the result agreed with the test data.

Past findings can be utilized for calculating the critical cooling times other than Δt_M: the prediction formula of Yurioka et al. can be utilized for calculating Δt_B, and that of Blondeau et al.[13] for Δt_{FP} and Δt_A. When these formulae are used without modification for expressing the influences of alloying elements, then Δt_B, Δt_{FP} and Δt_A are expressed as follows in a manner similar to Equation (24):

$$\begin{aligned}
&1\mathrm{n}(\Delta t_B) = 6.2CE_B + 0.87\\
&CE_B = C + \frac{Mn}{3.6} + \frac{Cu}{20} + \frac{Ni}{9} + \frac{Cr}{5} + \frac{Mo}{4} + 0.00501 \cdot 1\mathrm{n}(I'),
\end{aligned} \tag{25}$$

$$\begin{aligned}
&1\mathrm{n}(\Delta t_{FP}) = 8.74CE_{FP} - 0.19\\
&CE_{FP} = C + 0.28Mn + 0.053Ni + 0.36Cr + 0.42Mo + 0.0508 \cdot 1\mathrm{n}(I'),
\end{aligned} \tag{26}$$

$$\begin{aligned}
&1\mathrm{n}(\Delta t_A) = 0.99CE_A + 4.5\\
&CE_A = C + 1.14Mn + 1.06Ni + 2.02Cr + 2.33Mo + 0.21 \cdot 1\mathrm{n}(I'),
\end{aligned} \tag{27}$$

The value of I' in Equations (25) to (27) is the same as that in Equation (24), and its coefficients in these equations were determined in the same manner as in Equation (24) so that the values of the equations would agree with the measurement results of hardness distribution.

The following equations that appear in literatures can be used for calculating the hardness of the microstructures.

$$H_M = 884C\left(1 - 0.3C^2\right) + 294 \tag{28}$$

$$\begin{aligned}
&H_B = 197CE_{II} + 117\\
&CE_{II} = C + \frac{Si}{24} + \frac{Mn}{5} + \frac{Cu}{10} + \frac{Ni}{18} + \frac{Cr}{5} + \frac{Mo}{2.5} + \frac{V}{5} + \frac{Nb}{3}
\end{aligned} \tag{29}$$

$$H_{FP} = 90.9CE_{II} + 114 \tag{30}$$

Yurioka et al. proposed Equations (28) and (29)[9], and Okumura et al. Equation (30)[14]. When these values are given, hardness can be calculated from Equation (19).

Since it is necessary to introduce three parameters to be fitted to the experimental results into Equation (18), and determine the value of each of them for four critical cooling times as stated above, 12 parameter values in total have to be determined. As is clear from Equations (23) to (30), however, all the parameters to be determined in accordance with the experimental results are only those related to the influence of austenitic grain size, and because those terms have to conform to the conventional hardness estimation equations on the fusion line, the freedom in determining the parameter values is rather limited. The parameters that were determined in consideration of the experimental results in the present study were the coefficient of $\ln(I')$ in Equations (24) to (27), only four parameters in total, and all the other parameters were determined based on the past findings.

5.3 Prediction of hardness distribution from fusion line to Ac_3 line

Formulae for predicting hardness distribution from the fusion line (FL) to the Ac_3 line were discussed in Subsection 5.2. The Ac_3 temperature is indispensable for calculating hardness distribution, and it was obtained using the following equation[8]:

$$\begin{aligned}
1\mathrm{n}\left(Ac_3 - 273\right) = {} & 6.8165 - 0.47132C - 0.057321Mn + 0.066026Si\\
& - 0.050211Cr - 0.094455Ni + 0.10593Ti - 0.014847W + 2.0272N\\
& + 1.0536S - 0.12024SiC + 0.11629CrC - 0.30451MoMn\\
& + 0.68229MoSi - 0.21210MoCr + 0.12470NiC + 0.069960NiMn\\
& + 0.014003NiCr + 0.29225C^2 + 0.015660Mn^2 + 0.017315Cr^2\\
& + 0.46894Mo^2 + 0.0027897Ni^2
\end{aligned} \tag{31}$$

The fusion line was defined as a curve connecting positions where the maximum heating temperature was 1500°C. Note that the unit of Ac_3 temperature in Equation (31) is Kelvin (K).

Figs. 3 to 8 also compare the predicted and measured hardness distribution. It was necessary for the comparison to estimate not only hardness but also the shape and thermal history of the HAZ; the solution of welding heat transfer analysis proposed by Kasuya et al.[15] was used to calculate them. Figs. 3 to 8 show that the calculated hardness distribution agreed well with the experimental results except for those of Steel F. The calculated Ac_3 line was different from the measured one in some cases (such as Fig. 3 (e) and Fig. 5 (e)), but even in such cases, the difference in hardness was not large. The difference is presumably attributable to the estimation accuracy of welding heat transfer, and therefore, the improvement in the calculation accuracy of welding heat transfer will produce the improvement in the accuracy of hardness distribution prediction. However, because the object of the present study was to formulate equations for predicting the hardness at different positions of a HAZ, further details were not approached for heat transfer.

As the test data show, the highest hardness of Steel F was not obtained along the FL but at a position a little away from the FL. According to Equation (19), on the other hand, since the introduction of only the influence of austenitic grain size into the mechanism of hardness distribution, such a change in the position of the highest hardness does not occur. This indicates that the concept of the present study is applicable to Steels A to E, but not to Steel F.

Steel F contains boron and as is well known, boron has a significant effect on the hardenability of steel. As Equation (24) shows, we also weighted boron heavily in the present study in calculating the carbon equivalent. Koseki et al.[16] reported, however, that the effect of boron was largest not at the fusion line but at positions where the maximum heating temperature was far lower. As the reason for this, they pointed out that, at positions where the maximum heating temperature was about 1400°Csuch as those along the FL, nitrides would dissociate and free nitrogen resulting from the dissociation combine

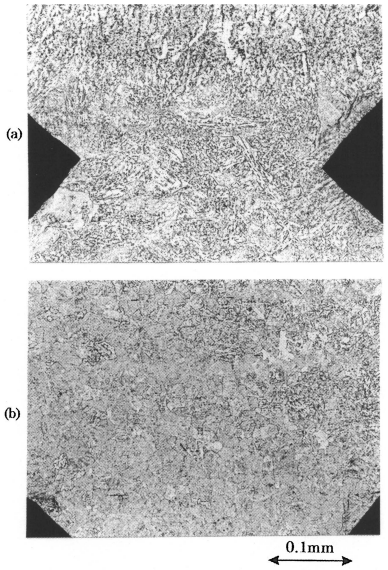

Fig. 9 Microstructures of Steel F after SAW(a: in the vicinity of fusion line, b: region of maximum hardness)

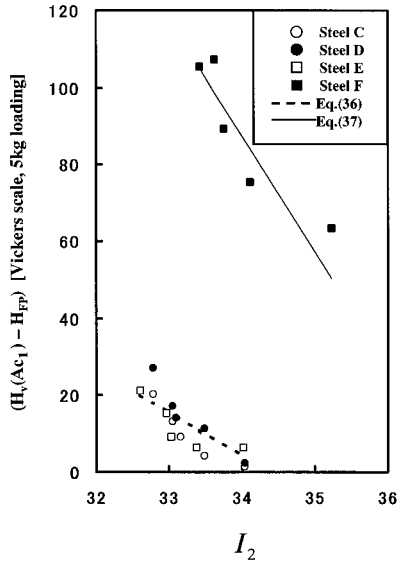

Fig. 10 Relationship between hardness at Ac_1 line and I_2

with boron during cooling, leading to a decrease in hardenability.

At positions where the maximum heating temperature is lower, nitrides do not dissociate and boron, working as free boron, serves to increase hardenability. **Fig. 9** shows microstructures of Steel F welded by the SAW at a position along the FL (part a) and the position where the hardness was highest (part b): the structure shown in part b is more hardened than that of part a; thus it is clear that the hardening effect is not necessarily highest along the FL. Because the equations used in the present study for estimating hardness were formulated in such a way that they agreed with past knowledge at the FL, and because the above behavior of boron was not a part of the past knowledge, the hardness prediction result for Steel F did not agree with the experimental data. This non-agreement is a subject of future study.

5.4 Prediction of hardness at Ac_1 line

The base metal structure along the Ac_1 line is considered to be tempered by the heat of welding, and for this reason, it is impossible to predict the hardness along the line by the method described earlier herein. Generally speaking, it is adequate to evaluate the change in hardness after tempering by using a temper parameter such as the one Okumura et al. used in the formula for predicting HAZ hardness after stress relieving [14]. However, since a temper parameter is calculated based on holding temperature and time of heat treatment, without modification, it is inapplicable to a process such as welding in which temperature changes with time. Such a problem occurs not only in welding but also in evaluating the effects of heating and cooling before and after tempering treatment. To solve the problem, Inoue[17] introduced the following parameter:

$$I_2 = \log\left(\sum_i 10^{\lambda_i}\right), \quad \lambda_i = \log(t) - \frac{Q_2}{2.3R}\frac{1}{T} + 50 \tag{32}$$

Equation (32) means that a welding thermal history is divided into a step function, and λ_i for each step is determined to calculate I_2. When the interval of each step is reduced, and Equation (32) becomes the form of integration as follows.

$$I_2 = 50 + \log\left[\int \exp(-Q_2/RT)\,dt\right] \tag{33}$$

This is in the same form as I in Equation (18). Note that for the average value of the activation energy Q_2, one was used that used by Inoue, that is,

$$Q_2 = 330{,}000 \text{ (J/mol)} \tag{34}$$

The following equation [8] was used to calculate the Ac_1 temperature, which was indispensable for the calculation:

$$\begin{aligned}1n\left(Ac_1 - 273\right) = {} & 6.5792 - 0.038058C + 0.052317Si + 0.011872Ni \\ & - 0.045575V + 0.18057Al + 0.011442W - 0.013403Cu + 5.5207B \\ & + 0.91209S - 1.1002P + 0.060014MnC - 0.096628CrC \\ & + 0.050625CrSi + 0.39802MoC - 0.34782MoMn + 0.40986MoSi \\ & - 0.12959MoCr - 0.048128NiC - 0.01090Mn^2 - 0.03550Si^2 \\ & + 0.010207Cr^2 + 0.36074Mo^2 - 0.0030705Ni^2\end{aligned} \tag{35}$$

Here, again, the unit of Ac_1 temperature in Equation (35) is Kelvin (K). A comparison was made to the hardness at Ac_1 with I_2 in Equation (33), and it was found that, as **Fig. 10** shows, their mutual relationship was roughly linear in each of the specimen steels. The relationship can be expressed as follows.

$$H_V(Ac_1) - H_{FP} = -11.1 \times I_2 + 382 \quad \text{(Steels C, D and E)} \tag{36}$$

$$H_V(Ac_1) - H_{FP} = -30.16 \times I_2 + 1113 \quad \text{(Steel F)} \tag{37}$$

Here, H_{FP} is given from Equation (30). Note that the right-hand side of either of these equations may become negative with a large value of I_2; in such a case, the value of the right-hand side is assumed to be zero, which means that the hardness at Ac_1 line cannot be lower than H_{FP}. The coefficients in the right-hand sides of Equations (36) and (37) are considered dependent on steel, but it was not possible to obtain a general solution applicable to any steel grades. Nevertheless, the present study is significant in showing the possibility of evaluating the influence of welding heat on HAZ hardness at Ac_1 line by using I_2 as shown in Fig. 10.

6. Summary

The present study began with examination of a carbon equivalent as an index of hardenability, then discussed what the mathematical forms of a carbon equivalent would be when the influence of austenitic grain size was taken into consideration by applying the additivity rule to the TTT diagram Kirkaldy et al. proposed, and finally attempted to formulate equations for predicting the hardness distribution in a HAZ of a weld joint. As a result, the present study yielded the following findings:

1) It is possible to introduce the influence of austenitic grain size into conventional carbon equivalents by adding a linear term of austenitic grain size number.
2) Using TTT curves in literatures, it was calculated that the carbon equivalent that expressed the critical cooling time in which a steel would transform into 100% martensite. The calculated carbon equivalent agreed well with that actually measured in hardness test of HAZs of weld joints.
3) Formulae for predicting hardness distribution were constructed by modifying the term of the austenitic grain size number into an integral form that could be operated using a welding thermal history and by introducing the influence of the austenitic grain size into the conventional method of hardness prediction. With respect to steels not containing boron, the predicted hardness distribution based on the developed formulae agreed well with that actually measured. The reason why the developed formulae were inapplicable to boron-containing steels is that, with such steels, the portion where the hardness is highest is not near the fusion line.
4) While the prediction of the hardness distribution mentioned in 3) above relates to the zone between the fusion line and the Ac_3 line, use of the temper parameter makes it possible to estimate the hardness at the Ac_1 line.

References

1) Grossmann, M.A.: Metal Progress. 4, 373(1938)
2) Dearden, J., H.O'Niell: Trans. Inst. Weld. 3, 203(1940)
3) Bastien, P.G., Dollet, J., Maynier, Ph.: Metal Constr. British Welding J. 9(1970)
4) Beckert, M., Hoiz, R.: Schweibtechnik. 23, 344(1973)
5) Kasuya, T., Yurioka, N.: Weld. J., 72, 263s(1993)
6) Kirkaldy, J.S., Thomson, B.A., Baganies, E.A.: In Hardenability Concept with Application to Steel. Edited by D.V.Doane, J.S.Kirkaldy, Warrendale, PA, AIME, 1978, p.82-125
7) Scheil, E.: Arc. Eisenhuttenwesen. 12, 565(1935)
8) Seyffarth, P.: Schweib-ZTU-Schaubilder. VEB, Berlin, Verlag Technik, 1982
9) Yurioka, N., Okumura, M., Kasuya, T., Cotton, H.: Metal Constr. 19, 217R(1987)
10) Ashby, M., Easterling, K.: Acta metall. 30, 1969(1982)
11) Ion, J., Earsterling, K., Ashby, M.: Acta Metall. 32, 1949(1984)
12) Ikawa, H., Oshige, H., Noi, S., Date, H., Uchikawa, K.: Trans. Japan Weld. Soc. 9, 47(1978)
13) Blondeau, R., Maynier, P., Dollet, J., Vieillard-Baron, B.: Heat Treatment'76, London, Metals Soc. 1976, p.189.
14) Okumura, M., Yurioka, N., Kasuya, T., Cotton, H.: Int. Conf. Residual Stress and Stress Relieving, IIW, Sofia, Bulgaria, 1987, p.61
15) Kasuya, T., Yurioka, N.: Weld. J. 72, 107s(1993)
16) Koseki, Sekiguchi, Tanabe, Inoue, Yamato: Preprints of the National Meeting of Japan Welding Society. 38, 1986, p.116
17) Inoue: Tetsu-to-Hagané. 66 (10), 1532 (1980)